



# Accuracy of intraoral scans of edentulous jaws with different generations of intraoral scanners compared to laboratory scans

Panagiotis Kontis<sup>1</sup>, Jan-Frederik Güth<sup>2</sup>, Oliver Schubert<sup>1</sup>, Christine Keul<sup>1\*</sup>

<sup>1</sup>Department of Prosthetic Dentistry, University Hospital, LMU Ludwig-Maximilians-University München, München, Germany

<sup>2</sup>Department of Prosthodontics, Center for Dentistry and Oral Health, Goethe University Frankfurt am Main, Germany

## ORCID

Panagiotis Kontis

<https://orcid.org/0000-0002-3334-3670>

Jan-Frederik Güth

<https://orcid.org/0000-0002-0693-0810>

Oliver Schubert

<https://orcid.org/0000-0002-2630-2635>

Christine Keul

<https://orcid.org/0000-0002-6710-8484>

**PURPOSE.** Purpose of this *in vitro* study was to determine the accuracy of different intraoral scans versus laboratory scans of impressions and casts for the digitization of an edentulous maxilla. **MATERIALS AND METHODS.** A PEEK model of an edentulous maxilla, featuring four hemispheres on the alveolar ridges in region 13, 17, 23 and 27, was industrially digitized to obtain a reference dataset (REF). Intraoral scans using Cerec Primescan AC (PRI) and Cerec AC Omnicam (OMN), as well as conventional impressions (scannable polyvinyl siloxane) were carried out (n = 25). Conventional impressions (E5I) and referring plaster casts were scanned with the inEOS X5 (E5M). All datasets were exported in STL and analyzed (Geomagic Qualify). Linear and angular differences were evaluated by virtually constructed measurement points in the centers of the hemispheres (P13, P17, P23, P27) and lines between the points (P17-P13, P17-P23, P17-P27). Kolmogorov-Smirnov test and Shapiro-Wilk test were performed to test for normal distribution, Kruskal-Wallis-H test, and Mann-Whitney-U test to detect significant differences in trueness, followed by 2-sample Kolmogorov-Smirnov test to detect significant differences in precision ( $P < .008$ ). **RESULTS.** Group PRI showed the highest trueness in linear and angular parameters ( $P < .001$ ), while group E5I showed the highest precision ( $P < .001$ ). **CONCLUSION.** Intraoral scan data obtained using Primescan showed the highest trueness while the indirect digitization of impressions showed the highest precision. To enhance the workflow, indirect digitization of the impression itself appears to be a reasonable technique, as it combines fast access to the digital workflow with the possibility of functional impression of mucosal areas. [J Adv Prosthodont 2021;13:316-26]

## KEYWORDS

Intraoral scanner; Laboratory scanner; Edentulous jaw; Digital impression; Accuracy

## Corresponding author

Christine Keul

Department of Prosthetic  
Dentistry, University Hospital,  
Ludwig-Maximilians-University  
München, Goethestrasse 70,  
Munich, Bayern, 80336, Germany  
Tel +49(0)89 4400 59571  
E-mail [Christine.Keul@med.uni-muenchen.de](mailto:Christine.Keul@med.uni-muenchen.de)

Received June 24, 2021 /

Last Revision September 2, 2021 /

Accepted October 5, 2021

© 2021 The Korean Academy of Prosthodontics

© This is an Open Access article distributed under the terms of the Creative Commons Attribution Non-Commercial License (<http://creativecommons.org/licenses/by-nc/4.0>) which permits unrestricted non-commercial use, distribution, and reproduction in any medium, provided the original work is properly cited.

## INTRODUCTION

Rapid development in computer aided design and computer aided manufacturing (CAD-CAM) has profoundly transformed dentistry and dental technology, and expanded the horizons in patient care and oral rehabilitation.<sup>1</sup> While fixed restorations have been successfully produced applying digital technologies for a long time, complete denture dentistry has begun to pass this transition only relatively late. Scientific effort has substantially accelerated after 2012, when Goodacre *et al.* reflected on the topic, correctly predicting that commercial digital complete denture fabrication should soon be available.<sup>2</sup> Shortly thereafter, Kattadiyil *et al.* presented a contribution introducing two commercially available systems, depicting specific characteristics and clinical protocols. As digital fabrication of dentures presents with intriguing aspects, such as enhanced time efficiency, the ease of reproducibility, and superior material properties, the issue has received strong impetus.<sup>3,4</sup> The undeniable virtues of the approach and most recent technological innovations, such as face scans, the virtual articulator, novel high-performance materials, and economical aspects have propelled digital complete dentistry to the forefront of clinical and scientific interest.<sup>5</sup> That is why numerous manufacturers provide systems or protocols for the digital fabrication of complete dentures, including computerized design, 3D printing of try-in dentures, and milling or 3D printing of denture bases or even the whole denture.<sup>6-8</sup>

However, complete denture fabrication still has specific obstacles in establishing comprehensive digital workflows and thus in suitability for implementation in clinical practice. These unresolved issues comprise the definition of certain functional and aesthetic parameters, the availability of reliable materials in additive manufacturing, and certain economic factors.<sup>5</sup> Besides the technical aspects, however, the clinical aspects so far haven't been in the focus of discussion. Above all, the reasonable direct digitization of the intraoral surfaces, representing the logical access to CAD-CAM related digital workflows, is questionable in complete denture treatment. In general, intraoral surface data can be acquired by either scanning the conventional impression or cast (indirect digitization), or

by intraoral scanning with an intraoral scanner (IOS) (direct digitization). Data acquired by IOS have proven to be as accurate as or even superior to conventional impressions for the fabrication of single crowns and fixed dental prostheses within a single quadrant,<sup>9,10</sup> and also for full arch impressions, which present clinically acceptable accuracy.<sup>11-13</sup> Although completely edentulous jaws are common in elderly patients, intraoral scanning has long been limited to tooth and implant supported fixed prostheses and to partially edentulous jaw sections.<sup>14</sup> Due to the absence of distinctive anatomical structures and the presence of large areas of non-attached mucosa, digital impressions of edentulous arches are particularly challenging for IOS systems and software.<sup>15-19</sup> For merging and overlaying of the single captured images of the IOS systems, distinct areas are required to avoid spatial torsion and warpage of the three-dimensional virtual model dataset.

Digital workflows for the fabrication of complete dentures have been established by different manufacturers and have been described and evaluated in clinical reports.<sup>5,20</sup> However, accomplishing a true functional impression is impeded, since tissue must be captured in varying motion-dependent situations.<sup>14,21</sup> Moreover, the accuracy of the digitization of edentulous jaws is not only pivotal in complete denture fabrication, but also most interesting regarding digital prosthetic planning, implant planning, and in patients for whom a conventional impression is difficult to perform.

Most of the research on the accuracy of direct and indirect digitization of edentulous anatomies, both *in vivo* and *in vitro*, is based on the calculation of surface differences between datasets after superimposition with the use of a best fit algorithm.<sup>22</sup> However, this method has been criticized for error underestimation caused by the alignment of datasets in a "most optimal" position, resulting in minimal distance between all data points, and therefore causing underestimation of the difference between the datasets.<sup>23</sup> These errors appear to be detrimental for comparisons of larger datasets, including edentulous arches.<sup>24</sup> On the other hand, a highly accurate dataset of the clinical situation, required for the calculation of reference geometries, is difficult to obtain *in vivo*, especially for

edentulous arches.

Therefore, the current *in vitro* study attempts to compare the accuracy, i.e., trueness and precision, of IOS and indirect digitization for an edentulous study model, using metric and angular deviations of the testing datasets compared to a highly accurate reference dataset using measurement points. The comparison of two relevant IOS systems of different generations intends to allow a comparison of the advancement of the IOS-technology.

The null hypotheses stated that (H01) IOS and indirect digitization exhibit no differences regarding accuracy of the obtained data, and (H02) no differences regarding accuracy can be found between the two generation of IOS devices.

## MATERIALS AND METHODS

An edentulous model of the upper jaw with four hemispheres of identical dimensions placed on the crest of the alveolar ridge (two hemispheres in the regions of the canines and two in the regions of the second molars) was digitally designed using reverse engineering software Geomagic Control 2015 (3D Systems, Valencia, CA, USA). On basis of this construction dataset, the testing model (Fig. 1) was milled from pink PEEK (PEEK Biosolution, LOT no 32116, Merz Dental GmbH, Lütjenberg, Germany) using the M5 Heavy Metal Milling Unit (Zirkonzahn GmbH, Gais, Italy). To obtain a



**Fig. 1.** PEEK testing model.

reference dataset (REF), the PEEK model was digitized using an optical 3D measurement system (InfiniteFocusG5, Alicona Imaging GmbH, Graz, Austria, objective 5x, resolution: finest topographic lateral = 3.51  $\mu\text{m}$ , vertical = 410 nm) and the resulting STL dataset (Fig. 2) was imported as reference into the software Control 2015.

The PEEK model was digitized with two intraoral scanners ( $n = 25/\text{group}$ ):

1. Cerec Primescan AC (Group PRI, Software Version 5.0.2, Sirona Dental Systems, Bensheim, Germany)
2. Cerec AC Omnicam (Group OMN, Software Version 4.5.2, Sirona Dental Systems, Bensheim, Germany)

All scans were performed by one skilled professional according to manufacturer's specifications. Before each scanning session, calibration of the scanning devices was conducted. An identical scanning strategy was performed with both IOS devices: starting at the maxillary tuberosity of the first quadrant, moving along the vestibular side of the alveolar ridge towards the second quadrant and then returning to the first quadrant crossing the palatal surface of the alveolar ridge, concluding with the palate area in a zigzag motion. To ensure an efficient and faithful capture of

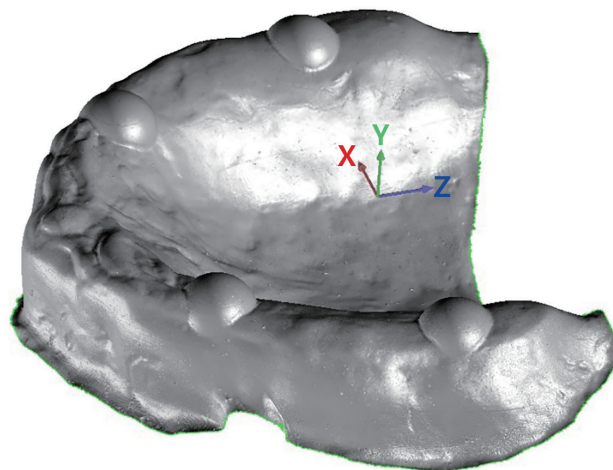


**Fig. 2.** Reference dataset [REF] aligned with the coordinate system. The XY-plane represents the sagittal plane whereas the transverse plane is depicted by the XZ-Plane. Consequently, the Y-axis reveals the vertical direction.

the anatomy, the scanning protocol was meticulously followed. However, instances of mismatch, especially between the hemispheres were observed frequently with Cerec Omnicam AC, which necessitated the removal and rescan of the affected areas using the system utility. The scan data were exported as STL files.

25 conventional impressions of the testing model were conducted employing double-mix impression technique with scannable polyvinyl siloxane impression material (Flexitime Fast & Scan light flow, LOT no K010022 and Flexitime Monophase Pro Scan, LOT no R010022; Kulzer GmbH, Hanau, Germany) using light cured custom impression trays (Palatray XL, LOT no A0984; Kulzer GmbH). All procedures were carried out according to the manufacturers' recommendations. The impressions were disinfected for two minutes (ORBI-Sept Impression Disinfection, LOT no A0984, Orbis Dental, Münster, Germany) according to the clinical protocol. Following a 24-hour storage period,

STL data of every impression were obtained by indirect digitization ( $n = 25$ ) using the In EOS X5 laboratory desktop scanner (group E5I, Software Version inLab SW 15.0, Sirona Dental Systems, Bensheim, Germany). Subsequently, all impressions were poured with a scannable Type IV plaster (Fino Scan Stone, LOT no 313096, FINO-Industrie Service GmbH, Brand-Erbisdorf, Germany), and the plaster casts were stored for another 24 hours. STL data of the plaster casts ( $n = 25$ ) were obtained using same laboratory desktop scanner (group E5M).

All datasets (REF and test datasets) were imported into Control 2015 software and post-processing was conducted. Only for a uniform spatial alignment of the datasets in the coordinate system, all test datasets were aligned with REF applying a best fit alignment on the hemispheres located in the canine areas and the area of the second right upper molar (Fig. 3).

Following the uniform alignment within the coordi-

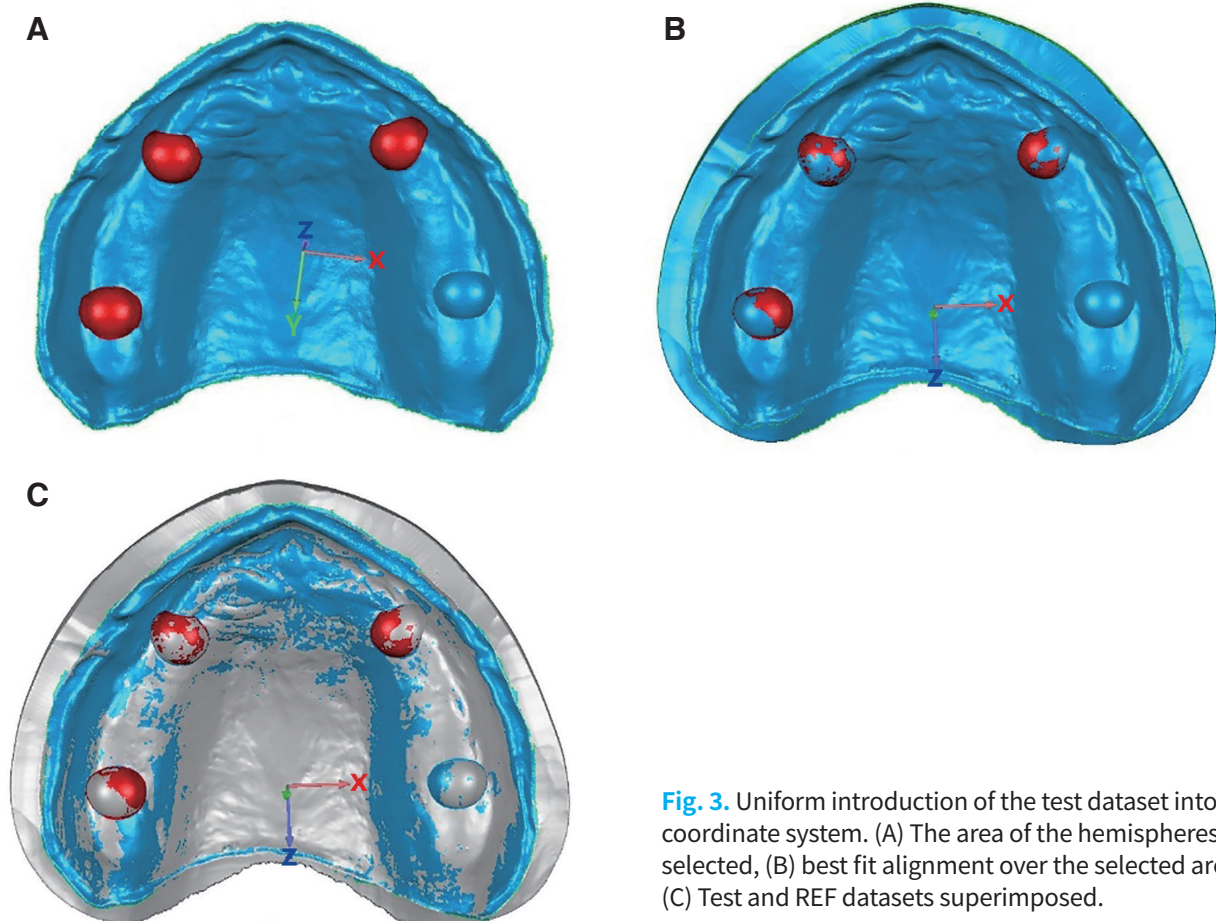


**Fig. 3.** Uniform introduction of the test dataset into the coordinate system. (A) The area of the hemispheres is selected, (B) best fit alignment over the selected area, (C) Test and REF datasets superimposed.



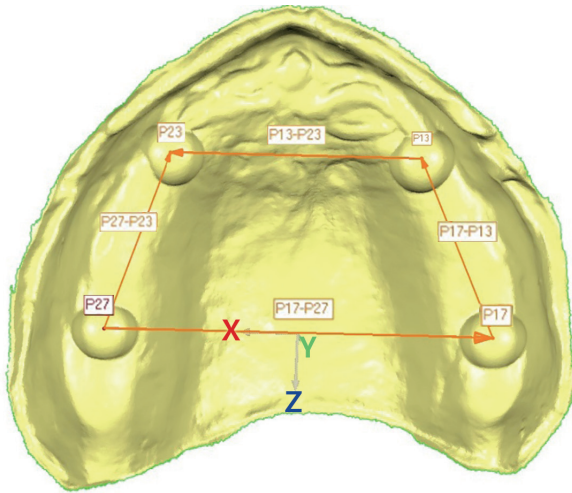


**Fig. 4.** Constructed points and vectors on the test dataset for the following calculation of the linear and angular aberrations.

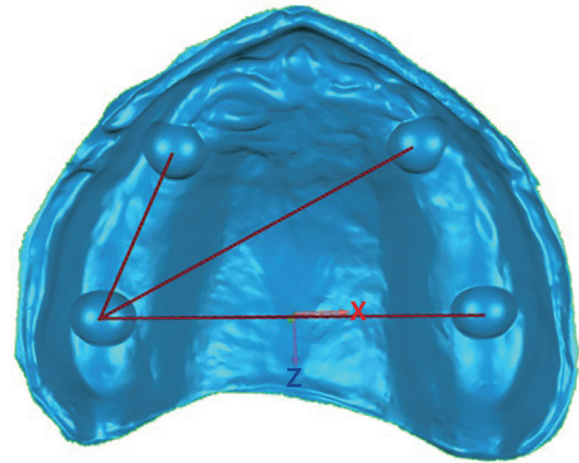


**Fig. 5.** Dataset aligned with the coordinate system and the measured distances.

nate system, the center of each hemisphere was identified to calculate the linear and angular aberrations of each test dataset. Therefore, a system function was used to automatically create four virtual points in the center of the hemispheres, named P17, P13, P23, and P27 (Fig. 4).

The point coordinates of P17, P13, P23, and P27, and vector coordinates of each of the four vectors P17-P13, P13-P23, P27-P23, and P17-P27 were imported into Microsoft Excel. Subsequently the distances P17-P13, P17-P23, P17-P27, and the angles between vector projections on the sagittal plane (YZ) and transverse plane (XZ) were calculated (Fig. 5). Capital letters X, Y, and Z denote the vector directions of the lines and lowercase letters x, y, and z describe the coordinates of the points in the X-, Y-, and Z-axes.

$$\text{Length of P17 - P13} = \sqrt{(x(P13) - x(P17))^2 + (y(P13) - y(P17))^2 + (z(P13) - z(P17))^2}$$

$$\text{Length of P17 - P23} = \sqrt{(x(P23) - x(P17))^2 + (y(P23) - y(P17))^2 + (z(P23) - z(P17))^2}$$

$$\text{Length of P17 - P27} = \sqrt{(x(P27) - x(P17))^2 + (y(P27) - y(P17))^2 + (z(P27) - z(P17))^2}$$

$$\text{Angle}_{\text{transverse}} = \arccos \frac{X(P17 - P13) \times X(P27 - P23) + Z(P17 - P13) \times Z(P27 - P23)}{\sqrt{X(P17 - P13)^2 + Z(P17 - P13)^2} \times \sqrt{X(P27 - P23)^2 + Z(P27 - P23)^2}} \times \frac{180}{\pi}$$

$$\text{Angle}_{\text{sagittal}} = \arccos \frac{Y(P17 - P13) \times Y(P27 - P23) + Z(P17 - P13) \times Z(P27 - P23)}{\sqrt{Y(P17 - P13)^2 + Z(P17 - P13)^2} \times \sqrt{Y(P27 - P23)^2 + Z(P27 - P23)^2}} \times \frac{180}{\pi}$$

The differences for each measured parameter between the test data and the REF data were calculated.

Statistical analysis was conducted applying SPSS Version 25 (SPSS Inc., Chicago, IL, USA). Kolmogorov-Smirnov test and Shapiro-Wilk test were applied to assess the normal distribution of the values, followed by Kruskal-Wallis-H test and post-hoc Mann-Whitney-U test to evaluate significant differences regarding trueness among groups. Significant differences in precision were examined with a two sample Kolmogorov-Smirnov test to investigate differences for the spreading of the test values. Bonferroni correction was applied for analysis of the trueness and the precision because of multiple testing. The level of significance was set at  $P = .008$ .

## RESULTS

Descriptive results, including median values, minimum and maximum, 95% confidence interval, mean values and standard deviation for each parameter are given in Table 1. Fig. 6 and Fig. 7 show the boxplots of all tested parameters. Fig. 8 depicts the mean trueness regarding measured distances in direct and indirect digitization, respectively.

Regarding distance P17-P13 groups PRI, E5I and OMN showed significantly higher trueness than group E5M ( $P < .001$ ). Considering distance P17-P23, significantly higher trueness was demonstrated by groups OMN and PRI ( $P < .001$  to  $P = .001$ ). For the distance P17-P27, group PRI presented the significantly highest trueness with OMN in the same value range ( $P < .001$ ). Regarding the angle on the sagittal plane (an-

gle YZ), significantly higher trueness was determined for groups PRI, E5M, and E5I ( $P < .001$  to  $P = .004$ ). In view of the angle on the transverse plane (angle XZ), groups E5M and PRI showed the best results ( $P < .001$  to  $P = .001$ ).

Regarding distance P17-P13 groups, E5I, PRI and OMN showed significantly higher precision than group E5M ( $P < .001$ ). Considering distance P17-P23, significantly higher precision was demonstrated by group E5I, followed by PRI in the same value range ( $P < .001$  to  $P = .001$ ). For the distance P17-P27, group E5I presented the significantly higher precision ( $P < .001$ ). Regarding angle on the sagittal plane (angle YZ), significantly higher precision was determined for groups E5I, PRI, and E5M ( $P < .001$  to  $P = .002$ ). In view of the angle on the transverse plane (angle XZ), group E5I showed the highest precision ( $P < .001$  to  $P = .001$ ).

**Table 1.** Descriptive statistics with median values (Median), minimum (Min), maximum (Max), 95% confidence interval (CI), mean values (Mean) and standard deviation (SD) for all tested parameters

		Direct digitization		Indirect digitization of the impression	Indirect digitization of the model
		PRI	OMN	E5I	E5M
Length aberration P17 - P13 (μm)	Median	-3.55 <sup>A/1</sup>	-6.92 <sup>A/1</sup>	-5.82 <sup>A/1</sup>	24.27 <sup>B/2</sup>
	Min/max	-37.69/24.17	-37.79/40.71	-31.89/279.81	-53.15/79.88
	95% CI	-11.17/0.12	-13.30/0.25	-19.43/28.59	15.57/35.81
	Mean ± SD	-5.52 ± 13.67	-6.52 ± 16.41	4.58 ± 58.16	25.69 ± 24.51
Length aberration P17 - P23 (μm)	Median	-10.30 <sup>A, B/1, 3</sup>	-3.90 <sup>B/3</sup>	-21.55 <sup>A/1</sup>	67.90 <sup>C/2</sup>
	Min/max	-45.09/48.65	-103.68/278.92	-36.26/587.00	-50.04/150.79
	95% CI	-17.32/2.03	-3.83/61.51	-48.00/52.78	54.55/81.73
	Mean ± SD	-7.64 ± 23.44	28.84 ± 79.15	2.39 ± 122.07	68.14 ± 32.92
Length aberration P17 - P27 (μm)	Median	2.31 <sup>B/3</sup>	37.43 <sup>B, C/3</sup>	-37.20 <sup>A/1</sup>	72.60 <sup>C/2</sup>
	Min/max	-65.70/57.72	-217.75/414.57	-61.69/632.60	-59.51/122.61
	95% CI	-8.10/14.88	20.08/140.84	-66.48/45.00	53.26/80.38
	Mean ± SD	3.39 ± 27.83	80.46 ± 146.27	-10.74 ± 135.04	66.82 ± 32.85
Angle sagittal YZ-plane (°)	Median	-0.01 <sup>A/1</sup>	0.10 <sup>B/2</sup>	-0.07 <sup>A/1</sup>	-0.03 <sup>A/1</sup>
	Min/max	-0.21/0.22	-0.21/0.89	-0.21/0.04	-0.22/0.58
	95% CI	-0.06/0.03	0.07/0.32	-0.09/-0.04	-0.11/0.04
	Mean ± SD	-0.01 ± 0.10	0.19 ± 0.30	-0.07 ± 0.06	-0.03 ± 0.18
Angle transverse XZ-plane (°)	Median	0.03 <sup>B, C/2</sup>	0.09 <sup>C/3</sup>	-0.09 <sup>A/1</sup>	-0.02 <sup>B/2</sup>
	Min/max	-0.12/0.17	-0.50/1.07	-0.17/-0.01	-0.20/0.08
	95% CI	0.00/0.06	0.06/0.32	-0.10/-0.06	-0.05/0.01
	Mean ± SD	0.03 ± 0.07	0.19 ± 0.32	-0.08 ± 0.05	-0.02 ± 0.07

Superscript letters indicate significant differences in trueness, superscript numbers indicate significant differences in precision.

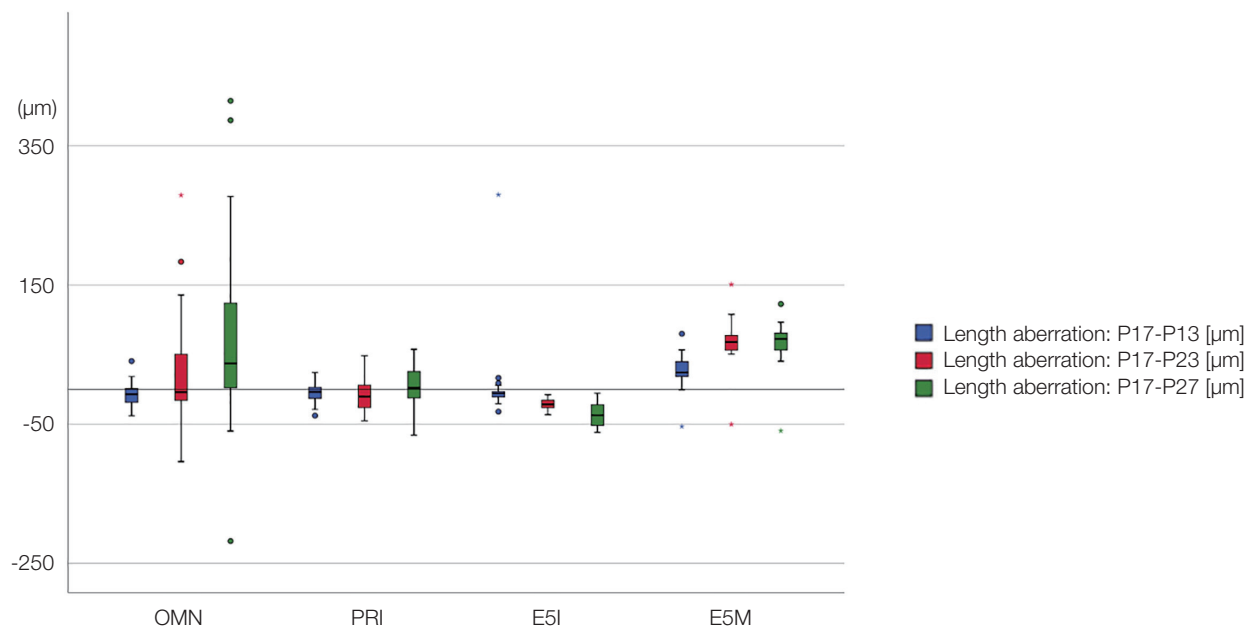


**Fig. 6.** Boxplots for linear parameters (μm).

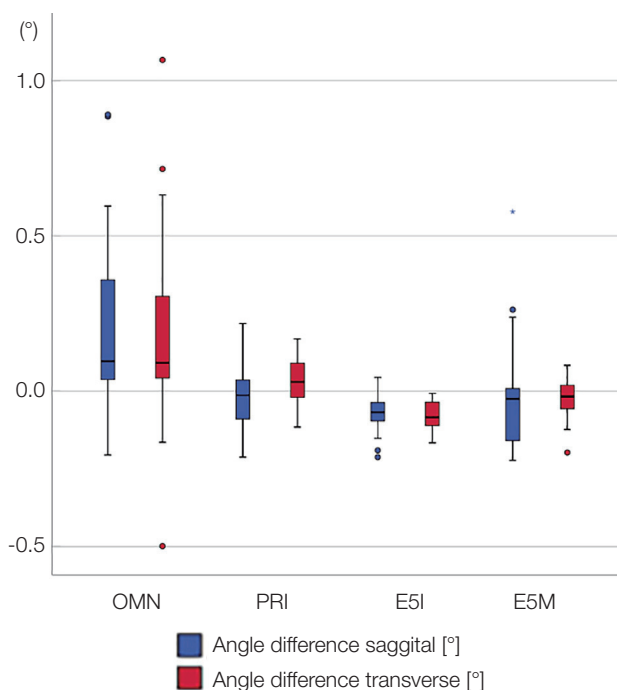


**Fig. 7.** Boxplots for angular parameters (°).

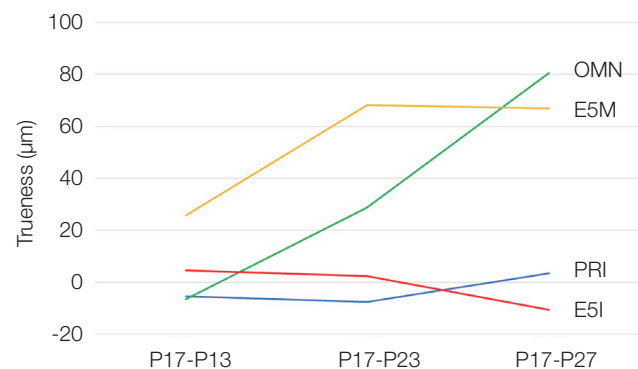


**Fig. 8.** Mean trueness of digitization methods by linear distances.

## DISCUSSION

This investigation aimed to compare the *in vitro* accuracy of different direct and indirect computer aided impression techniques for edentulous jaws regarding linear and angular warpage in the resulting virtual models. Therefore, linear distances between the centers of hemispheres and angular parameters between

the connection lines of the hemisphere-centers were examined.

The first null hypothesis (H01), stating that no significant differences between direct and indirect digitization should arise, has to be rejected. The highest trueness was observed for intraoral scanning using the Cerec Primescan while the highest precision was revealed for the indirect digitization of the impression with the In EOS X5 laboratory scanner.

The group PRI presented a larger angle in the XZ plane in conjunction with an increased P17-P27 distance, signifying a transverse expansion of the scan data in the posterior part of the edentulous arch. By contrast, the decrease in value of the XZ angle in combination with increased distances P17-13, P17-P23, and P17-P27 exhibited by group E5M can be explained by the torsion of the two hemi arches along the Z-axis in the transverse plane. Group OMN showed higher values in both the XZ and XY angles, reflecting torsion in both the sagittal and transverse dimension. In group E5I, a posterior contraction occurred primarily in the transverse plane. Moreover, regarding distance P17-P27, both IOS revealed lower precision compared to indirect digitization of cast and impression with the In EOS X5, indicating that IOS may present lower predictability in their results as the size of overlapped data increases.

Nedelcu *et al.* found a posterior expansion and anterior contraction of a completely dentate arch for Cerec AC Omnicam.<sup>13</sup> Regarding examinations with a similar experimental setup, Kuhr *et al.*<sup>25</sup> measured higher vertical angle deviations for Cerec AC Omnicam compared to Trios 3 and True Definition on a fully dentate model. Several authors have discussed the correlation between the increase of horizontal error and growing scanned distance across the edentulous arch.<sup>26-29</sup> This phenomenon is attributed to a progressive error culmination in the stitching process of single images. To determine the angular and linear aberrations in the present study, four spherical geometries were integrated in the testing model. The hemispheres were placed on an area of low resilience in patients (alveolar ridge) so that differences between the current *in vitro* results and *in vivo*, pertaining to the resilience of the tissue, could be minimized. By optical 3D measurement using the InfiniteFocusG5

reference measurement system, the three-dimensional position of these reference hemispheres was determined prior to data acquisition. As larger parts of the arch are captured, and greater numbers of images must be overlapped, inaccuracies accumulate, increasing the overall distortion of the generated data.<sup>28,30,31</sup> In contrary, digitization applying laboratory desktop scanners does not reveal a comparable deviation pattern. Since laboratory scanners capture large parts of the model or impression simultaneously, the effect of error culmination is minimized.<sup>29</sup> Contrary to the present results, the digitization of completely dentate stone models has been found to be more accurate than the direct digitization of impressions.<sup>32</sup> This difference could be attributed to the geometry of the testing model, as impressions of edentulous arches present fewer complex geometries to capture with scarcely any undercuts, rendering the recording with optical scanners less demanding.<sup>33,34</sup> At the same time, the absence of undercuts alleviates the occurrence of distortions during impression setting and removal. Presently, indirect digitization of the impression performed similarly to direct digitization with Primescan in most of the measured parameters, confirming previous observations by Chebib *et al.*<sup>35</sup> on Trios 3 and digitized polyvinylsiloxane impressions of an edentulous maxilla.

Furthermore, Cerec Primescan AC and Cerec AC Omnicam demonstrated significant differences in trueness for angle YZ and in precision for both measured angles. Thus, the second null hypothesis (H02) predicting that no significant differences between the two IOS would be found has to be rejected. This observation may be due to the different recording technology of the two intraoral scanning systems. While the Cerec AC Omnicam is working on basis of the optical triangulation and confocal microscopy, the Cerec Primescan AC is working on an optical measurement principle on basis of shortwave light with optical high frequency contrast analysis for dynamic depth scan and high-resolution sensors. The investigated systems worked on basis of the same software, but with different versions. This might be a second argument for the difference in some of the measured parameters. The investigated Cerec AC Omnicam was due to the year of manufacture not appropriate for



installation of the same software version as for the Cerec Primescan AC. Further investigations should be accordingly adapted to investigate the same software version. This is one of the limitations of the present study.

Most researchers attempt to visualize spatial distortions of digital models by using three-dimensional color-coded difference images after best-fit alignment.<sup>11-13,31,35,36</sup> Therefore, comparison of the results with the results of preceding studies is challenging as the present study is based on the virtual measurement of real geometries without applying a best fit alignment among the datasets. A best fit alignment was only used to ensure a uniform orientation of all datasets within the three-dimensional coordinate system. Hence, the measurement of real linear and angular deviations is one of the benefits of the present measurement and analysis design. However, the findings of the present study can be compared with results of prior investigations on edentulous jaws applying a comparable methodology (e.g., linear error measurement between implants or implant like objects). Braian and Wennerberg<sup>37</sup> reported larger errors (0.023 mm within a quadrant, 0.061 mm diagonally and 0.193 mm across the arch) for Cerec AC Omnicam in digitizing an edentulous mandible. In another investigation, the researchers found no statistical differences between Cerec Primescan AC and Cerec AC Omnicam regarding the distances between scan bodies on an edentulous maxilla.<sup>38</sup>

The minimum necessary accuracy in complete denture fabrication is defined by the tissue displacement caused by the denture, which has been reported to be in a range of 1,270 - 1,770  $\mu\text{m}$ .<sup>39</sup> Concerning this aspect, all investigated methods produce clinically acceptable results. Relating to the direct digitization of edentulous jaws, one must also note that no intraoral scanning device is able to produce a true functional impression with border molding. Nonetheless, without functional extension of the mucosal border and compression of the highly resilient posterior palatal areas, a reliable marginal and palatal seal cannot be established, which, in turn, could negatively affect denture retention,<sup>35</sup> although the merit of such peripheral and palatal seal has yet to be substantiated by research.<sup>40</sup> On the other hand, according to

the mucostatic principle, denture retention can be achieved through surface tension between denture base and underlying tissues.<sup>41</sup> The exceptional fit of CAM manufactured dentures, combined with the superior accuracy of IOS, may result in a more intimate contact between the denture's intaglio surfaces and the underlying mucosa.<sup>7,18</sup> These factors can usefully contribute to denture retention and help qualify some of the above-mentioned drawbacks. Consequently, a thorough recording of border extension and mucosal resilience does not seem to be as imperative with modern approaches.

Due to the design of the testing model, the digitization accuracy of the functional border was not the aim of the present study and must therefore be considered a limitation. Constructing and introducing reference objects in the mobile mucous membrane should be a topic of further analyses. However, the design of the study allowed for explicit comparison of the generations of IOSs regarding their capacity to capture large areas of edentulous intraoral surfaces as the analysis of the linear distances in combination with angle measurement can provide comprehensive information about the pattern of distortion generated by the different scanning systems.

Generally, reports on dentures fabricated in a digital workflow are ambiguous regarding the level of retention and patient satisfaction.<sup>17,18</sup> By contrast, digitization of functional impressions and casted models ensures the establishment of a proper marginal seal,<sup>35</sup> produces more accurate results<sup>12</sup> and enables a direct access to the digital workflow.

The present study was conducted in a laboratory setting and each step was executed in accordance with clinical specifications by the same skilled professional. Although the feasibility or time efficiency of the scanning process was not the part of the study, the fact that the Cerec AC Omnicam frequently produced mismatch during scanning which necessitated rescan must additionally remind when comparing the generations or methodologies and estimating their suitability to digitize edentulous jaws.

However, with the laboratory settings some limitations have to be mentioned. The ambient light is different from *in vivo* data acquisition. Both investigated systems offer the opportunity to choose between

the *in vitro* and the *in vivo* acquisition mode. To standardize the light conditions a special light box should be used for further investigations. As color of the testing model, a gingiva-like color was chosen. However, the refractive index of scanned substrate may have an influence on the accuracy of the acquired data. Opposed to this, *in vivo* experiments might be influenced by multiple factors such as patient movement, patient compliance, and the presence of saliva. In addition, a non-reflective surface of the PEEK analyzing model might have helped improve the results of the intraoral scanners in the present study.<sup>28</sup>

The results of the present study can be relevant regarding clinical application and future scientific effort. On basis of the above clinical considerations the scanning of the functional impression with a laboratory scanner could be considered at the moment as the most reliable method for the digitization of edentulous arches.

## CONCLUSION

Within its limitations, results of the present study suggest that, regarding trueness, direct digitization with the Primescan presented best values, followed by the indirect digitization of the conventional impression using the In EOS X5. In view of precision, the indirect digitization of the conventional impression using the In EOS X5 showed superior results. If a functional impression is required, the indirect digitization for a conventional elastomeric impression might be the most reasonable access point to the digital workflow.

## REFERENCES

1. Beuer F, Schweiger J, Edelhoff D. Digital dentistry: an overview of recent developments for CAD/CAM generated restorations. *Br Dent J* 2008;204:505-11.
2. Goodacre CJ, Garbacea A, Naylor WP, Daher T, Marchack CB, Lowry J. CAD/CAM fabricated complete dentures: concepts and clinical methods of obtaining required morphological data. *J Prosthet Dent* 2012;107:34-46.
3. Al-Fouzan AF, Al-Mejrad LA, Albarrag AM. Adherence of *Candida* to complete denture surfaces in vitro: a comparison of conventional and CAD/CAM complete dentures. *J Adv Prosthodont* 2017;9:402-8.
4. Srinivasan M, Gjengedal H, Cattani-Lorente M, Mousa M, Durual S, Schimmel M, Müller F. CAD/CAM milled complete removable dental prostheses: an in vitro evaluation of biocompatibility, mechanical properties, and surface roughness. *Dent Mater J* 2018;37:526-33.
5. Schweiger J, Stumbaum J, Edelhoff D, Güth JF. Systematics and concepts for the digital production of complete dentures: risks and opportunities. *Int J Comput Dent* 2018;21:41-56.
6. Kattadiyil MT, Goodacre CJ, Baba NZ. CAD/CAM complete dentures: a review of two commercial fabrication systems. *J Calif Dent Assoc* 2013;41:407-16.
7. Baba NZ, AlRumaih HS, Goodacre BJ, Goodacre CJ. Current techniques in CAD/CAM denture fabrication. *Gen Dent* 2016;64:23-28.
8. Steinmassl PA, Klaunzer F, Steinmassl O, Dumfahrt H, Grunert I. Evaluation of currently available CAD/CAM denture systems. *Int J Prosthodont* 2017;30:116-22.
9. Güth JF, Keul C, Stimmelmayer M, Beuer F, Edelhoff D. Accuracy of digital models obtained by direct and indirect data capturing. *Clin Oral Investig* 2013;17:1201-8.
10. Keul C, Stawarczyk B, Erdelt KJ, Beuer F, Edelhoff D, Güth JF. Fit of 4-unit FDPs made of zirconia and Co-Cr-alloy after chairside and labside digitalization-a laboratory study. *Dent Mater* 2014;30:400-7.
11. Malik J, Rodriguez J, Weisbloom M, Petridis H. Comparison of accuracy between a conventional and two digital intraoral impression techniques. *Int J Prosthodont* 2018;31:107-13.
12. Ender A, Attin T, Mehl A. In vivo precision of conventional and digital methods of obtaining complete-arch dental impressions. *J Prosthet Dent* 2016;115:313-20.
13. Nedelcu R, Olsson P, Nyström I, Rydén J, Thor A. Accuracy and precision of 3 intraoral scanners and accuracy of conventional impressions: a novel in vivo analysis method. *J Dent* 2018;69:110-8.
14. Hack G, Liberman L, Vach K, Tchorz JP, Kohal RJ, Patzelt SBM. Computerized optical impression making of edentulous jaws - an in vivo feasibility study. *J Prosthodont Res* 2020;64:444-53.
15. Fang JH, An X, Jeong SM, Choi BH. Development of complete dentures based on digital intraoral impressions - Case report. *J Prosthodont Res* 2018;62:116-20.
16. Goodacre BJ, Goodacre CJ. Using intraoral scanning to fabricate complete dentures: first experiences. *Int J*

- Prosthodont 2018;31:166-70.
17. Goodacre BJ, Goodacre CJ, Baba NZ. Using intraoral scanning to capture complete denture impressions, tooth positions, and centric relation records. *Int J Prosthodont* 2018;31:377-81.
  18. Lo Russo L, Salamini A. Single-arch digital removable complete denture: a workflow that starts from the intraoral scan. *J Prosthet Dent* 2018;120:20-4.
  19. Unkovskiy A, Wahl E, Zander AT, Huettig F, Spintzyk S. Intraoral scanning to fabricate complete dentures with functional borders: a proof-of-concept case report. *BMC Oral Health* 2019;19:46.
  20. Schweiger J, Güth JF, Edelhoff D, Stumbaum J. Virtual evaluation for CAD-CAM-fabricated complete dentures. *J Prosthet Dent* 2017;117:28-33.
  21. Patzelt SB, Vonau S, Stampf S, Att W. Assessing the feasibility and accuracy of digitizing edentulous jaws. *J Am Dent Assoc* 2013;144:914-20.
  22. Rasaie V, Abduo J, Hashemi S. Accuracy of intraoral scanners for recording the denture bearing areas: a systematic review. *J Prosthodont* 2021;30:520-39.
  23. O'Toole S, Osnes C, Bartlett D, Keeling A. Investigation into the accuracy and measurement methods of sequential 3D dental scan alignment. *Dent Mater* 2019;35:495-500.
  24. Güth JF, Edelhoff D, Schweiger J, Keul C. A new method for the evaluation of the accuracy of full-arch digital impressions in vitro. *Clin Oral Investig* 2016;20:1487-94.
  25. Kuhr F, Schmidt A, Rehmann P, Wöstmann B. A new method for assessing the accuracy of full arch impressions in patients. *J Dent* 2016;55:68-74.
  26. Iturrate M, Eguiraun H, Etxaniz O, Solaberrieta E. Accuracy analysis of complete-arch digital scans in edentulous arches when using an auxiliary geometric device. *J Prosthet Dent* 2019;121:447-54.
  27. Giménez B, Özcan M, Martínez-Rus F, Pradíes G. Accuracy of a digital impression system based on parallel confocal laser technology for implants with consideration of operator experience and implant angulation and depth. *Int J Oral Maxillofac Implants* 2014;29:853-62.
  28. van der Meer WJ, Andriessen FS, Wismeijer D, Ren Y. Application of intra-oral dental scanners in the digital workflow of implantology. *PLoS One* 2012;7:e43312.
  29. Fukazawa S, Odaira C, Kondo H. Investigation of accuracy and reproducibility of abutment position by intraoral scanners. *J Prosthodont Res* 2017;61:450-9.
  30. Andriessen FS, Rijkens DR, van der Meer WJ, Wismeijer DW. Applicability and accuracy of an intraoral scanner for scanning multiple implants in edentulous mandibles: a pilot study. *J Prosthet Dent* 2014;111:186-94.
  31. Renne W, Ludlow M, Fryml J, Schurch Z, Mennito A, Kessler R, Lauer A. Evaluation of the accuracy of 7 digital scanners: An in vitro analysis based on 3-dimensional comparisons. *J Prosthet Dent*. 2017;118:36-42.
  32. Keul C, Güth JF. Accuracy of full-arch digital impressions: an in vitro and in vivo comparison. *Clin Oral Investig* 2020;24:735-45.
  33. Persson AS, Odén A, Andersson M, Sandborgh-Englund G. Digitization of simulated clinical dental impressions: virtual three-dimensional analysis of exactness. *Dent Mater* 2009;25:929-36.
  34. DeLong R, Pintado MR, Ko CC, Hodges JS, Douglas WH. Factors influencing optical 3D scanning of vinyl polysiloxane impression materials. *J Prosthodont* 2001;10:78-85.
  35. Chebib N, Kalberer N, Srinivasan M, Maniewicz S, Perneger T, Müller F. Edentulous jaw impression techniques: an in vivo comparison of trueness. *J Prosthet Dent* 2019;121:623-30.
  36. Imburgia M, Logozzo S, Hauschild U, Veronesi G, Mangano C, Mangano FG. Accuracy of four intraoral scanners in oral implantology: a comparative in vitro study. *BMC Oral Health* 2017;17:92.
  37. Braian M, Wennerberg A. Trueness and precision of 5 intraoral scanners for scanning edentulous and dentate complete-arch mandibular casts: a comparative in vitro study. *J Prosthet Dent* 2019;122:129-36.e2.
  38. Mangano FG, Admakin O, Bonacina M, Lerner H, Rutkunas V, Mangano C. Trueness of 12 intraoral scanners in the full-arch implant impression: a comparative in vitro study. *BMC Oral Health* 2020;20:263.
  39. Lytle RB. Soft tissue displacement beneath removable partial and complete dentures. *J Prosthet Dent* 1962;12:34-43.
  40. Carlsson GE, Ortorp A, Omar R. What is the evidence base for the efficacies of different complete denture impression procedures? a critical review. *J Dent* 2013;41:17-23.
  41. Bohannon HM. A critical analysis of the mucostatic principle. *J Prosthet Dent* 1954;4:232-41.